Amino-Functionalized Trisilylmethanes: Precursors for a New Class of Tripodal Amido Ligands in Transition Metal Complexes[†]

Harald Memmler and Lutz H. Gade*

Institut für Anorganische Chemie der Universität Würzburg, Am Hubland, 97074 Würzburg, Germany

Joseph W. Lauher

Department of Chemistry, State University of New York, Stony Brook, New York 11794

Received February 3, 1994[®]

A series of amino-functionalized trisilylmethanes $HC(SiMe_2NHR)_3$ [R = 4-$CH_3C_6H_4$ (**1**), 3-$CH_3C_6H_4$ (**2**), 2-$CH_3C_6H_4$ (**3**), C_6H_5 (**4**), 4-FC_6H_4 (**5**), $HC\{SiMe_2NH[(S)-CH(CH_3)Ph]\}_3$ (**8**)] has been synthesized and studied structurally both in solution and in the solid state. The temperature dependence of the chemical shift of the apical proton in **1–5** and **8** along with ^1H-NOESY experiments at variable temperature have established solution structures in which the peripheral groups point in, respectively, opposite directions relative to the ligand framework. The structural arrangement of the amines in the solid state was established by single-crystal X-ray structure analyses of **1** and **8**. **1**: monoclinic, $P2_1/n$, $a = 9.160(2)$ Å, $b = 9.456(3)$ Å, $c = 35.25(1)$ Å, $\beta = 94.23(2)°$, $Z = 4$, $V = 3044.6(6)$ Å^3, $R = 0.043$. **8**: trigonal, $P3$, $a = 16.510(2)$ Å, $c = 10.592(2)$ Å, $Z = 3$, $V = 2500.4(5)$ Å^3, $R = 0.047$. Whereas **1** has an almost inverted structure as postulated in solution, the amino-functionalized trisilylmethane unit in **8** may be viewed as part of an adamantane-related structure. The corresponding trilithium amides were obtained readily by reaction with n-butyllithium and, on the basis of their ^1H- and ^{13}C-NMR spectra, are thought to have an adamantoid cage structure. They react with $TiX_4(THF)_2$ to yield the tripodal amidotitanium complexes $HC(SiMe_2NR)_3TiX$ {R = 4-$CH_3C_6H_4$, X = Cl [Br] (**14a** [**b**]), R = 3-$CH_3C_6H_4$, X = Cl [Br] (**15a** [**b**]), R = 4-FC_6H_4, X = Br (**16**)} which are of interest as monofunctional building blocks in more complicated structural arrays.

Introduction

There has recently been a burgeoning interest in the development of formally highly charged polydentate ligands due to their ability to stabilize large sectors in the coordination sphere of high valent early transition metal complexes.[1-7] The reactivity of a transition metal complex is thereby limited to a remaining reactive site occupied by ligands which may be substituted readily or removed completely. Amides, in particular, have been successfully employed to this end since their good σ- and π-donor capabilities meet the electronic requirements of highly Lewis acidic metal centers.[8] Moreover, since amido ligands are disubstituted at the donor atom, their incorporation into a polydentate ligand system enables the variation (and thus control) of both the ligand framework and the periphery, an opportunity not offered by, e.g., alkoxides. The most prominent example of the versatility of this concept is the structural chemistry and chemical reactivity of a series of azatrane complexes studied in the groups of Verkade,[2,3]

Schrock,[4-6] Arnold,[7] and others.[9] The extreme exploitation of the steric demand of the tren-derived [tren = tris(2-aminoethyl)-amine] amido ligand is a common feature of most of the systems studied to date and has been the key to unusual coordination geometries or the stabilization of highly reactive molecular fragments in their coordination sphere.[6,7]

The stabilization of a high valent early transition metal by a polydentate ligand appeared to us to provide the key to a general strategy for the use of such complex fragments in polynuclear coordination compounds in which the reactive site is masked either by a bridging ligand or, preferably, a metal-metal bond.[10] For this purpose a series of trifunctional amines has been synthesized[11,12] which may serve as precursors to mixed amido halides with a more open structure, and thus fewer steric constraints, than the above-mentioned azatrane systems (Figure 1).[13,14] The tripodal amido ligands of amides A–C are formally trianionic species with a neopentane,[11,13] trisilylmethane,[12] and trisilylsilane framework[15] while D is dianionic due to the replacement of a negatively charged amido function by a neutral tertiary amino function (2-pyridyl).[14]

The chemistry of functionalized trisilylmethanes has thus far received little attention outside the context of basic research in silane chemistry.[16-19] The only previous attempt to prepare tripodal amido complexes based on an amino-functionalized trisilylmethane was reported by Bürger and co-workers who

---

[†] We dedicate this paper to Professor Helmut Werner on the occasion of his 60th birthday.

[®] Abstract published in *Advance ACS Abstracts*, June 1, 1994.

(1) Verkade, J. G. *Acc. Chem. Res.* **1993**, *26*, 483.

(2) (a) Naiini, A. A.; Menge, W. M. P. B.; Verkade, J. G. *Inorg. Chem.* **1991**, *30*, 5009. (b) Menge, W. M. P. B.; Verkade, J. G. *Inorg. Chem.* **1991**, *30*, 4628.

(3) (a) Plass, W.; Verkade, J. G. *J. Am. Chem. Soc.* **1992**, *114*, 2275. (b) Plass, W.; Verkade, J. G. *Inorg. Chem.* **1993**, *32*, 3762.

(4) Cummins, C. C.; Schrock, R. R.; Davis, W. M. *Organometallics* **1992**, *11*, 1452.

(5) Cummins, C. C.; Lee, J.; Schrock, R. R.; Davis, W. M. *Angew. Chem., Int. Ed. Engl.* **1992**, *31*, 1501.

(6) Cummins, C. C.; Schrock, R. R.; Davis, W. M. *Angew. Chem., Int. Ed. Engl.* **1993**, *32*, 756.

(7) Cristou, V.; Arnold, J. *Angew. Chem., Int. Ed. Engl.* **1993**, *32*,

(8) (a) Lappert, M. F.; Power, P. P.; Sanger, A. R.; Srivastava, R. C. *Metal and Metalloid Amides*; Ellis Horwood-Wiley: Chichester, England, 1980. (b) Bradley, D. C.; Chisholm, M. H. *Acc. Chem. Res.* **1976**, *9*, 273. (c) Chisholm, M. H.; Rothwell, I. P. In *Comprehensive Coordination Chemistry*; Wilkinson, G., McCleverty, J. A., Gillard, R. D., Eds.; Pergamon Press: Oxford, 1987; Vol. 2.

(9) Schubart, M.; O'Dwyer, L.; Gade, L. H.; Li, W.-S.; McPartlin, M. *Inorg. Chem.*, in press.

(10) Friedrich, S.; Memmler, H.; Gade, L. H.; Li, W.-S.; McPartlin, M. *Angew. Chem., Int. Ed. Engl.* **1994**, *33*, 676.

(11) Gade, L. H.; Mabr, N. *J. Chem. Soc., Dalton Trans.* **1993**, 489.

(12) Gade, L. H.; Becker, C.; Lauher, J. W. *Inorg. Chem.* **1993**, *32*, 2308.

(13) Friedrich, S.; Gade, L. H.; Edwards, A. J.; McPartlin, M. *Chem. Ber.* **1993**, *126*, 1797.

(14) Friedrich, S.; Gade, L. H.; Edwards, A. J.; McPartlin, M. *J. Chem. Soc., Dalton Trans.* **1993**, 2861.

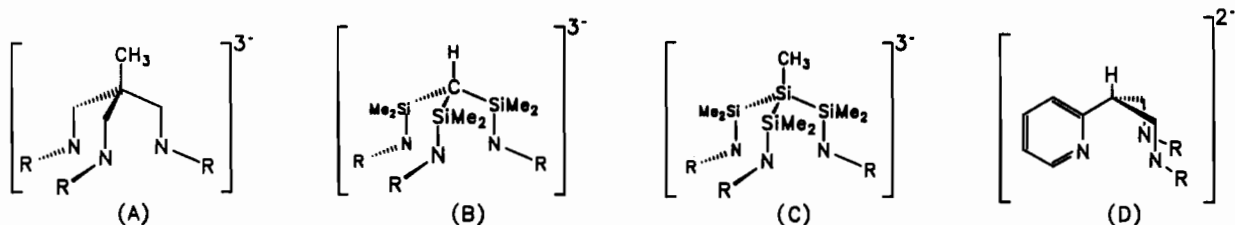(15) Schubart, M.; Findeis, B.; Gade, L. H.; McPartlin, M. submitted for publication.

Figure 1. Tripodal amido ligands coordinated to tetravalent transition metals.

prepared $HC(SiMe_2NHMe)_3$ but were not successful in coordinating this ligand precursor to a transition metal.[20] This failure was interpreted by the authors as a consequence of incomplete lithiation of the amine in the first step of their synthesis. In the light of our recent study of the chemistry of trisilylmethane-derived multifunctional lithium amides,[12] which has indeed revealed a high degree of cooperativity in this metalation reaction, the original interpretation appears questionable. It may, however, be due to the thermal lability of Bürger's amine precursor that amide complexes were not obtained at the time.

Here we report the synthesis of a series of novel amino-functionalized trisilylmethanes which are precursors to type **B** ligands, the investigation of their structures in solution and in the solid state, their metalation, and coordination to Ti(IV) centers.

Experimental Section

All manipulations were performed under an inert gas atmosphere of dried argon in standard (Schlenk) glassware which was flame dried with a Bunsen burner prior to use. Solvents were dried according to standard procedures and saturated with Ar. The deuterated solvents used for the NMR spectroscopic measurements were degassed by three successive "freeze–pump–thaw" cycles and dried over 4-Å molecular sieves.

The ^{1}H-, ^{13}C-, ^{29}Si-, and ^{19}F-NMR spectra were recorded on a Bruker AC 200 spectrometer equipped with a B-VT-2000 variable temperature unit (at 200.13, 50.32, 39.76 and 188.31 MHz, respectively) with tetramethylsilane and $CFCl_3$ as references. The ^{1}H-NOESY spectra were recorded using the Bruker automation program NOESY (absolute magnitude mode). A total of 128 1K-FID's of 16 scans over a sweep width of 800–1000 Hz (depending on the sample) were collected; the mixing times were set at 0.5, 1.5, and 3.0 s, which were varied randomly within a range of ± 25 ms to suppress *J*-cross peaks. The F1 dimension was zero-filled to 512 W prior to apodization (unshifted sine bell) and Fourier transformation. All 2D spectra were symmetrized. Infrared spectra were recorded on Perkin Elmer 1420 and Bruker IRS 25 FT-spectrometers.

Elemental analyses were carried out in the microanalytical laboratory of the Chemistry Department at Würzburg. Due to the moisture sensivity of the compounds some elemental analyses deviated by more than 0.4% from the calculated values. $HC(SiMe_2Br)_3$,[12,18] $TiCl_4(THF)_2$,[21] and $TiBr_4(THF)_2$[21] were prepared according to literature procedures. The primary amines employed in the ligand syntheses were distilled before use. All other chemicals used as starting materials were obtained commercially and used without further purification.

Preparation of Compounds. General Procedure for the Synthesis of the Amino-Functionalized Trisilylmethanes. Over a period of 2 h a solution of $HC(SiMe_2Br)_3$ (21.4 g = 0.05 mol) in diethyl ether was added to a stirred mixture of 0.15 mol of the respective primary amine and triethylamine (22 mL = 0.16 mol) in 250 mL of diethyl ether, which was cooled at 0 °C with an ice bath. Subsequently, the reaction mixture was stirred at room temperature for 14 h, the triethyl ammonium bromide

removed by filtration through a G3 frit and the solvent of the filtrate evaporated *in vacuo*. The colorless residue was dissolved in 30 mL of diethyl ether and the solution stored at –40 °C to yield the tripodal amines as highly crystalline colorless solids.

$HC\{SiMe_2NH(4-CH_3C_6H_4)\}_3$ (**1**). Yield: 76%. Mp: 102 °C. Anal. Calcd for $C_{28}H_{43}N_3Si_3$: C, 66.47; H, 8.58; N, 8.31. Found: C, 66.89; H, 9.04; N, 8.40. ^{1}H-NMR (CDCl$_3$, 295 K): δ = 0.47 (s, Si(CH_3)$_2$), 0.83 (s, HC(Si···)$_3$), 2.31 (s, 4-CH_3C$_6$H$_4$), 3.63 (s, NH), 6.44 (d, $^3J_{HH}$ = 6.4, H^{2,6}), 6.93 (d, H^{3,5}). {^{1}H}^{13}C-NMR (CDCl$_3$, 295 K): δ = 2.7 (Si(CH_3)$_2$), 3.6 (HC(Si···)$_3$), 20.4 (4-CH_3C$_6$H$_4$), 116.4, 126.6, 129.9, 143.9 (C^2, C^4, C^3, C^1 of 4-CH$_3$C$_6$H$_4$). {^{1}H}^{29}Si-NMR (CDCl$_3$, 295 K): δ = 1.2. IR (KBr): 3395 (m), 3380 (m), 3024 (w), 3008 (w), 2959 (m), 2913 (m), 2860 (w), 1612 (s), 1511 (vs), 1441 (m), 1365 (s), 1287 (vs), 1212 (s), 1204 (s), 1182 (w), 1117 (w), 1019 (s), 898 (s), 851 (vs), 811 (vs), 722 (s), 643 (m) cm^{-1}.

$HC\{SiMe_2NH(3-CH_3C_6H_4)\}_3$ (**2**). Yield: 73%. Mp: 114 °C. Anal. Calcd for $C_{28}H_{43}N_3Si_3$: C, 66.47; H, 8.58; N, 8.31. Found: C, 67.03; H, 8.55; N, 8.41. ^{1}H-NMR (CDCl$_3$, 295 K): δ = 0.45 (s, Si(CH_3)$_2$), 0.77 (s, HC(Si···)$_3$), 2.20 (s, 3-CH_3C$_6$H$_4$), 3.65 (s, NH), 6.33 (d, $^3J_{H^4H^5}$ = 6.4, H^4), 6.35 (H^2), 6.56 (d, $^3J_{H^5H^6}$ = 7.6, H^6), 6.98 (dd, H^5). {^{1}H}^{13}C-NMR (CDCl$_3$, 295 K): δ = 2.8 (Si(CH_3)$_2$), 4.7 (HC(Si···)$_3$), 21.5 (3-CH_3C$_6$H$_4$), 113.3, 117.4, 118.7, 129.2, 139.1, 146.5 (C^6, C^4, C^2, C^5, C^3, C^1 of 3-CH$_3$C$_6$H$_4$). {^{1}H}^{29}Si-NMR (CDCl$_3$, 295 K): δ = 0.9. IR (hexanes): 3400 (w), 3347 (w), 1608 (vs), 1590 (m), 1493 (m), 1362 (m), 1294 (s), 1259 (s), 1173 (m), 1091 (w), 1008 (s), 950 (m), 860 (vs), 839 (vs), 772 (s), 689 (m) cm^{-1}.

$HC\{SiMe_2NH(2-CH_3C_6H_4)\}_3$ (**3**). Yield: 69%. Mp: 111 °C. Anal. Calcd for $C_{28}H_{43}N_3Si_3$: C, 66.47; H, 8.58; N, 8.31. Found: C, 67.15; H, 8.70; N, 8.30. ^{1}H-NMR (CDCl$_3$, 295 K): δ = 0.43 (s, Si(CH_3)$_2$), 0.92 (s, HC(Si···)$_3$), 2.02 (s, 2-CH_3C$_6$H$_4$), 3.47 (s, NH), 6.49 (d, $^3J_{H^3H^4}$ = 8.0, H^3), 6.63 (ddd, $^3J_{H^5H^6}$ = 7.4, $^3J_{H^5H^4}$ = 7.3, $^4J_{H^5H^3}$ = 1.1, H^5), 6.83 (ddd, $^4J_{H^4H^6}$ = 1.6, H^4), 7.01 (d, H^6). {^{1}H}^{13}C-NMR (CDCl$_3$, 295 K): δ = 2.9 (Si(CH_3)$_2$), 4.1 (HC(Si···)$_3$), 17.9 (2-CH_3C$_6$H$_4$), 114.8, 117.6, 123.6, 127.0, 130.6, 144.8 (C^6, C^4, C^2, C^5, C^3, C^1 of 2-CH$_3$C$_6$H$_4$). {^{1}H}^{29}Si-NMR (CDCl$_3$, 295 K): δ = 1.4. IR (KBr): 3420 (m sh), 3408 (m), 3020 (m), 2965 (m), 1600 (s), 1576 (s), 1490 (vs), 1464 (m), 1443 (m), 1380 (s), 1366 (m), 1287 (s), 1263 (s), 1200 (s), 1177 (m), 1155 (w), 1107 (m), 1048 (s), 1005 (v)s, 901 (vs), 845 (vs), 798 (s), 770 (s), 743 (vs), 682 (m), 639 (w) cm^{-1}.

$HC\{SiMe_2NH(C_6H_5)\}_3$ (**4**). Yield: 63%. Mp: 56 °C. Anal. Calcd for $C_{25}H_{37}N_3Si_3$: C, 64.74; H, 8.04; N, 9.10. Found: C, 64.36; H, 8.21; N, 8.98. ^{1}H-NMR (CDCl$_3$, 295 K): δ = 0.46 (s, Si(CH_3)$_2$), 0.93 (s, HC(Si···)$_3$), 3.67 (s, NH), 6.49 (ddd, $^3J_{H^3H^4}$ = 7.3, $^4J_{H^2H^6}$ = 1.6, $^4J_{H^2H^4}$ = 1.2, H^{2,6}), 6.75 (tt, H^4), 7.12 (ddd, $^3J_{H^3H^4}$ = 6.6, $^4J_{H^3H^5}$ = 1.6, H^{3,5}). {^{1}H}^{13}C-NMR (CDCl$_3$, 295 K): δ = 2.7 (Si(CH_3)$_2$), 3.4 (HC(Si···)$_3$), 116.4, 117.7, 129.4, 146.4 (C^{2,6}, C^4, C^{3,5}, C^1 of C$_6$H$_5$). {^{1}H}^{29}Si-NMR (CDCl$_3$, 295 K): δ = 0.8. IR (KBr): 3491 (m), 3480 (m), 3038 (w), 2977 (w), 2900 (w), 1602 (vs), 1498 (vs), 1475 (s), 1379 (s), 1293 (vs), 1268 (s), 1257 (s), 1181 (m), 1152 (w), 1078 (m), 1013 (s), 1003 (s), 900 (vs), 891 (vs), 976 (s), 845 (vs), 775 (s), 703 (vs), 696 (vs), 648 (w) cm^{-1}.

$HC\{SiMe_2NH(4F-C_6H_4)\}_3$ (**5**). Yield: 61%. Mp: 70 °C. Anal. Calcd for $C_{25}H_{34}F_3N_3Si_3$: C, 57.99; H, 6.62; N, 8.12. Found: C, 57.95; H, 7.02; N, 7.80. ^{1}H-NMR (CDCl$_3$, 295 K): δ = 0.36 (s, Si(CH_3)$_2$), 0.80 (s, HC(Si···)$_3$), 3.49 (s, NH), 6.28–6.35, 6.70–6.79 (m, 4-FC$_6$H$_4$). {^{1}H}^{13}C-NMR (CDCl$_3$, 295 K): δ = 2.6 (Si(CH_3)$_2$), 3.2 (HC(Si···)$_3$), 115.8 (d, $^2J_{FC}$ = 22.3), 117.1 (d, $^3J_{FC}$ = 7.4), 142.5, 155.9 (d, $^1J_{FC}$ = 235.9) (C^{2,6}, C^4, C^{3,5}, C^1 of 4-FC$_6$H$_4$). {^{1}H}^{29}Si-NMR (CDCl$_3$, 295 K): δ = 1.4. {^{1}H}^{19}F-NMR (CDCl$_3$, 295 K): δ = –127.9. IR (KBr): 3380 (m, br), 2958 (w), 1625 (w), 1505 (vs), 1449 (m), 1361 (m), 1289 (s), 1258 (s), 1250 (s), 1162 (m), 1097 (w), 1020 (s), 1014 (s), 891 (vs), 868 (vs), 840 (s), 815 (vs), 789 (s), 695 (w), 646 (w) cm^{-1}.

$HC\{SiMe_2NH[(S)-CH(CH_3)Ph]\}_3$ (**8**). Yield: 65%. Mp: 40 °C. Anal. Calcd for $C_{31}H_{49}N_3Si_3$: C, 67.95; H, 9.12; N, 7.67. Found: C,

(16) (a) Merker, R. L.; Scott, M. J. *J. Org. Chem.* **1964**, *29*, 953. (b) Merker, R. L.; Scott, M. J. *J. Organomet. Chem.* **1965**, *4*, 98. (c) Sakurai, H.; Tominaga, K.; Watanabe, T.; Kumada, M. *Tetrahedron Lett.* **1966**, 5493.

(17) (a) Eaborn, C.; Hitchcock, P. B.; Lickiss, P. D. *J. Organomet. Chem.* **1984**, *269*, 235. (b) Hager, R.; Steigelmann, O.; Müller, G.; Schmidbaur, H. *Chem. Ber.* **1989**, *122*, 2115 and references cited therein.

(18) Eaborn, C.; Hitchcock, P. B.; Lickiss, P. D. *J. Organomet. Chem.* **1983**, *252*, 281.

(19) Baier, M.; Bissinger, P.; Schmidbaur, H. *Z. Naturforsch., B* **1993**, *48*, 1672.

(20) Bürger, H.; Mellies, R.; Wiegel, K. *J. Organomet. Chem.* **1977**, *142*, 55.

(21) Manzer, L. E. *Inorg. Synth.* **1982**, *21*, 135.

68.19; H, 9.58; N, 7.43. ^{1}H-NMR (C_6D_6, 295 K): $\delta = -0.88$ (s, *HC*-(SiMe$_2$)$_3$), 0.13, 0.24 (s, Si(C*H$_3$*)$_2$), 1.25 (d, $^3J_{HH} = 6.8$, 2-C*H$_3$*), 1.79 (d, $^3J_{HH} = 9.9$, N*H*), 3.92 (dq, C*H*Me), 7.04–7.22 (m, C_6H_5). {^{1}H}^{13}C-NMR (C_6D_6, 295 K): $\delta = 3.6$, 4.0 (Si(C*H$_3$*)$_2$), 5.2 (*HC*(Si···)$_3$), 27.8. (2-*CH$_3$*), 52.0 (*HC*Me), 126.2, 126.6, 128.6, 149.5 (C^{2,6}, C^4, C^{3,5}, C^1 of C_6H_5). {^{1}H}^{29}Si-NMR (C_6D_6, 295 K): $\delta = 1.0$. IR (KBr): 3343 (s), 3083 (w), 3062 (m), 3023 (s), 2960 (vs), 2922 (s), 2898 (s), 2869 (m), 1604 (w), 1492 (s), 1453 (vs), 1409 (vs), 1370 (s), 1296 (m), 1252 (vs), 1202 (s), 1123 (vs), 1061 (s), 1030 (vs), 951 (vs), 815 (vs), 700 (vs), 678 (s) cm^{-1}.

General Procedure for the Synthesis of the Amidotitanium Complexes HC(SiMe$_2$NR)$_3$TiX (R = 4-CH$_3$-C$_6$H$_4$, 3-CH$_3$-C$_6$H$_4$, 4-FC$_6$H$_4$; X = Cl, Br). To a solution of HC(SiMe$_2$NHR)$_3$ (5.0 mmol) in 30 mL of pentane and 2 mL of Et$_2$O, which was cooled at −50 °C, were added 6 mL of a 2.5 M *n*-BuLi/*n*-hexane solution. The reaction mixture was warmed to room temperature and subsequently stirred for ca. 4 h. After completion of the lithiation, the reaction mixture was then cooled to −50 °C, solid TiX$_4$(THF)$_2$ (5.4 mmol; X = Cl, Br) added, and then the mixture was warmed to room temperature over a period of 20 h. Removal of the solvent *in vacuo*, extraction of the residue with 20 mL of toluene and filtration through a G3 frit yielded a deep red filtrate which was concentrated to 10 mL and stored at −40 °C for crystallization of the product. The titanium complexes were isolated as orange-red (X = Cl) and deep red (X = Br) crystalline solids.

Spectroscopic Data for the Solvated Lithium Salts (Not Isolated). HC{SiMe$_2$N(Li)(4-CH$_3$C$_6$H$_4$)}$_3$·2Et$_2$O (10). ^{1}H-NMR (C_6D_6, 295 K): $\delta = -0.80$ (s, *HC*(Si···)$_3$), 0.56 (s, Si(C*H$_3$*)$_2$), 0.58 (t, $^3J_{HH} = 7.4$, OCH$_2$C*H$_3$*), 2.21 (s, 4-C*H$_3$*C$_6$H$_4$), 2.71 (q, OC*H$_2$*CH$_3$), 6.74 (d, $^3J_{HH} = 8.2$, H^{2,6}), 6.92 (d, H^{3,5}). {^{1}H}^{13}C-NMR (C_6D_6, 295 K): $\delta = 6.9$ (Si(C*H$_3$*)$_2$), 9.9 (*HC*(Si···)$_3$), 14.1 (OCH$_2$*CH$_3$*), 20.6 (4-*CH$_3$*C$_6$H$_4$), 64.2 (O*CH$_2$*CH$_3$), 121.8, 123.6, 130.6, 156.0 (C^2, C^4, C^3, C^1 of 4-CH$_3$C$_6$H$_4$).

HC{SiMe$_2$N(Li)(3-CH$_3$C$_6$H$_4$)}$_3$·2Et$_2$O (11). ^{1}H-NMR (C_6D_6, 295 K): $\delta = -0.81$ (s, *HC*(Si···)$_3$), 0.55 (s, Si(C*H$_3$*)$_2$), 0.56 (t, $^3J_{HH} = 7.0$, OCH$_2$C*H$_3$*), 2.18 (s, 3-C*H$_3$*C$_6$H$_4$), 2.72 (q, OC*H$_2$*CH$_3$), 6.41–7.03 (m, 3-CH$_3$C$_6$*H$_4$*). {^{1}H}^{13}C-NMR (C_6D_6, 295 K): $\delta = 6.9$ (Si(C*H$_3$*)$_2$), 10.1 (*HC*(Si···)$_3$), 14.1 (OCH$_2$*CH$_3$*), 21.9 (3-*CH$_3$*C$_6$H$_4$), 64.2 (O*CH$_2$*CH$_3$), 116.4, 119.0, 122.7, 130.0, 139.2, 158.5 (C^6, C^4, C^2, C^5, C^3, C^1 of 3-*CH$_3$*C$_6$H$_4$).

HC{SiMe$_2$N(Li)[(S)-CH(CH$_3$)Ph]}$_3$·2THF (12). ^{1}H-NMR (C_6D_6, 295 K): $\delta = -0.72$ (s, *HC*(Si···)$_3$), 0.16, 0.27 (s, Si(C*H$_3$*)$_2$), 1.25 (d, $^3J_{HH} = 6.8$, 2-C*H$_3$*), 1.42 (m, OCH$_2$C*H$_2$*), 3.58 (m, O*CH$_2$*CH$_2$) 3.92 (q, C*H*Me), 7.04–7.22 (m, C_6H_5). {^{1}H}^{13}C-NMR (C_6D_6, 295 K): $\delta = 3.6$, 4.0 (Si(C*H$_3$*)$_2$), 6,8 (*HC*(Si···)$_3$), 25.6. (2-*CH$_3$*), 27.9 (O*CH$_2$*CH$_2$), 52.3 (*HC*Me), 67.8 (m, O*CH$_2$*CH$_2$), 126.3, 126.6, 128.6, 149.6 (C^{2,6}, C^4, C^{3,5}, C^1 of C_6H_5).

Spectroscopic and Analytical Data for the Ti–Amides. HC{SiMe$_2$N-(4-CH$_3$C$_6$H$_4$)}$_3$TiCl (14a). Yield 35%. Anal. Calcd for C$_{28}$H$_{40}$ClN$_3$Si$_3$Ti: C, 57.37; H, 6.88; N, 7.17. Found: C, 57.02; H, 6.51; N, 6.88. ^{1}H-NMR (C_6D_6, 295 K): $\delta = -0.25$ (s, *HC*(Si···)$_3$), 0.39 (s, Si-(C*H$_3$*)$_2$), 2.08 (s, 4-C*H$_3$*C$_6$H$_4$), 6.97 (d, $^3J_{HH} = 8.1$ Hz, H^2), 7.05 (d, H^3). {^{1}H}^{13}C-NMR (C_6D_6, 295 K): $\delta = 4.0$ (Si(C*H$_3$*)$_2$), 9.4 (*HC*(Si···)$_3$), 20.8 (4-*CH$_3$*C$_6$H$_4$), 122.9, 131.0, 133.2, 148.5 (C^2, C^3, C^4, C^1 of 4-CH$_3$C$_6$H$_4$). {^{1}H}^{29}Si-NMR (C_6D_6, 295 K): $\delta = 6.2$. IR (Nujol): 1492 (m), 1255 (m), 1237 (w), 1225 (w), 1213 (w), 1091 (w), 1013 (w), 978 (w), 900 (w), 891 (w), 865 (w), 843 (s), 806 (s), 719 (w) cm^{-1}.

HC{SiMe$_2$N(4-CH$_3$C$_6$H$_4$)}$_3$TiBr (14b). Yield 55%. Anal. Calcd for C$_{28}$H$_{40}$BrN$_3$Si$_3$Ti(630.67): C, 53.32; H, 6.36; N, 6.66. Found: C, 53.49; H, 6.42; N, 6.38. ^{1}H-NMR (C_6D_6, 295 K): $\delta = -0.28$ (s, *HC*(Si···)$_3$), 0.37 (s, Si(C*H$_3$*)$_2$), 2.07 (s, 4-C*H$_3$*C$_6$H$_4$), 6.98 (d, $^3J_{HH} = 8.2$, H^2), 7.10 (d, H^3). {^{1}H}^{13}C-NMR (C_6D_6, 295 K): $\delta = 3.8$ (Si(C*H$_3$*)$_2$), 9.9 (*HC*(Si···)$_3$), 20.8 (4-*CH$_3$*C$_6$H$_4$), 123.1, 130.3, 133.4, 148.1 (C^2, C^3, C^4, C^1 of 4-CH$_3$C$_6$H$_4$). {^{1}H}^{29}Si-NMR (C_6D_6, 295 K): $\delta = 6.5$. IR (Nujol): 1673 (m), 1490 (w), 1253 (s), 1200 (m), 1130 (m), 1087 (s), 1012 (vs), 961 (w), 885 (w), 864 (w), 838 (m), 798 (vs), 670 (m) cm^{-1}.

HC{SiMe$_2$N(3-CH$_3$C$_6$H$_4$)}$_3$TiCl (15a). Yield 41%. Anal. Calcd for C$_{28}$H$_{40}$ClN$_3$Si$_3$Ti: C, 57.37; H, 6.88; N, 7.17. Found: C, 57.13; H, 6.67; N, 7.01. ^{1}H-NMR (C_6D_6, 295 K): $\delta = -0.26$ (s, *HC*(Si···)$_3$), 0.41 (s, Si(C*H$_3$*)$_2$), 2.11 (s, 3-C*H$_3$*C$_6$H$_4$), 6.59–7.13 (m, 3-CH$_3$C$_6$*H$_4$*). {^{1}H}^{13}C-NMR (C_6D_6, 295 K): $\delta = 3.8$ (Si(C*H$_3$*)$_2$), 9.2 (*HC*(Si···)$_3$), 21.5 (3-*CH$_3$*C$_6$H$_4$), 120.1, 123.5, 124.8, 129.5, 139.3, 151.0 (C^2, C^4, C^5, C^6, C^3, C^1 of 3-CH$_3$C$_6$H$_4$). {^{1}H}^{29}Si-NMR (C_6D_6, 295 K): $\delta = 6.3$. IR (Nujol): 1592 (s), 1573 (w), 1262 (s), 1251 (vs), 1090 (w), 1016 (m), 986 (m), 950 (w), 899 (m), 865 (s), 850 (s), 832 (vs), 799 (m), 780 (w), 726 (m), 694 (m) cm^{-1}.

Table 1. Crystal Data and Experimental Details for **1** and **8**

	1	**8**
empirical formula	C$_{28}$H$_{43}$N$_3$Si$_3$	C$_{31}$H$_{49}$N$_3$Si$_3$
fw	505.92	548.00
cryst syst	monoclinic	trigonal
cell params		
a (Å)	9.160(2)	16.510(2)
b (Å)	9.456(3)	10.592(2)
c (Å)	35.25(1)	
V (Å^3)	3044.6(6)	2500.4(5)
β (deg)	94.23	
Z	4	3
D_{calc} (g cm^{-1})	1.104	1.092
space group	$P2_1/n$	$P3$
$F(000)$	1096	894
μ(Cu Kα) (cm^{-1})^a	15.79	14.73
2θ(max) (deg)	69.9	110.9
no. of observns with $I > 3.00\sigma(I)^b$	1016	1090
no. of variables^c	319	333
residuals: R; R_w	0.043; 0.047	0.047; 0.044
goodness of fit	2.22	1.50
largest peak in final diff map (e Å^{-3})	0.16	0.17

^{a} An empirical absorption correction, using the program DIFABS (Walker, N.; Stuart, D. *Acta Crystallogr. A* **1983**, *39*, 158) was applied for both crystals. The data were corrected for Lorentz and polarization effects. ^{b} The intensities of the representative reflections were measured every 60 min of X-ray exposure time. They remained constant throughout the data collection, indicating in both cases crystal and electronic stability (no decay correction was applied). ^{c} Neutral atom scattering factors were taken from: Cromer, D. T.; Waber, J. T. *International Tables of X-ray Crystallography*; The Kynoch Press: Birmingham, England, 1974; Vol. IV, Table 2.2A. Anomalous dispersion effects were included in the final F_{calc} (Ibers, J. A.; Hamilton, W. C. *Acta Crystallogr.* **1964**, *17*, 781).

HC{SiMe$_2$N(3-CH$_3$C$_6$H$_4$)}$_3$TiBr (15b). Yield 22%. Anal. Calcd for C$_{28}$H$_{40}$BrN$_3$Si$_3$Ti: C, 53.32; H, 6.36; N, 6.66. Found: C, 53.14; H, 6.12; N, 6.55. ^{1}H-NMR (C_6D_6, 295 K): $\delta = -0.28$ (s, *HC*(Si···)$_3$), 0.40 (s, Si(C*H$_3$*)$_2$), 2.12 (s, 3-C*H$_3$*C$_6$H$_4$), 6.69–7.13 (m, 3-CH$_3$C$_6$*H$_4$*). {^{1}H}^{13}C-NMR (C_6D_6, 295 K): $\delta = 4.5$ (Si(C*H$_3$*)$_2$), 10.4 (*HC*(Si···)$_3$), 22.1 (3-*CH$_3$*C$_6$H$_4$), 121.0, 124.4, 125.6, 130.1, 139.9, 151.2 (C^2, C^4, C^5, C^6, C^3, C^1 of 3-CH$_3$C$_6$H$_4$). {^{1}H}^{29}Si-NMR (C_6D_6, 295 K): $\delta = 6.5$. IR (Nujol): 1593 (m), 1574 (w), 1378 (vs), 1304 (w), 1253 (vs), 1165 (m), 1092 (m), 1018 (m), 972 (w), 950 (w), 904 (w), 852 (s), 833 (vs), 808 (m), 736 (w), 696 (w) cm^{-1}.

HC{SiMe$_2$N(4-FC$_6$H$_4$)}$_3$TiBr (16). Yield: 34%. Anal. Calcd for C$_{25}$H$_{31}$BrF$_3$N$_3$Si$_3$Ti: C, 57.99; H, 6.62; N, 8.12. Found: C, 57.54; H, 6.86; N, 7.89. ^{1}H-NMR (C_6D_6, 295 K): $\delta = -0.41$ (s, *HC*(Si···)$_3$), 0.24 (s, Si(C*H$_3$*)$_2$), 6.40–7.10 (m, 4-FC$_6$*H$_4$*). {^{1}H}^{13}C-NMR (C_6D_6, 295 K): $\delta = 3.5$ (Si(C*H$_3$*)$_2$), 8.3 (*HC*(Si···)$_3$), 116.3 (d, $^2J_{FC} = 22.4$ Hz), 124.5 (d, $^3J_{FC} = 7.5$ Hz), 146.5, 160.0 (d, $^1J_{FC} = 243.4$ Hz) (C^{2,6}, C^{3,5}, C^1, C^4 of 4-FC$_6$H$_4$). {^{1}H}^{29}Si-NMR (C_6D_6, 295 K): $\delta = 6.6$. {^{1}H}^{19}F-NMR (C_6D_6, 295 K): $\delta = -119.2$. IR (Nujol): 1490 (vs), 1268 (m), 1235 (m sh), 1220 (s), 1161 (w), 1105 (m), 1028 (m), 985 (w), 902 (m), 883 (vs), 860 (vs), 852 (s), 837 (vs), 756 (m), 735 (m), 710 (w) cm^{-1}.

X-ray Crystallographic Study of 1 and 8. The clear, colorless crystals of **1** had a block-shaped prismatic habit while those of **8** had a regular trigonal habit. A fragment of a crystal of **1** with the approximate dimensions 0.500 × 0.300 × 0.200 mm was mounted under argon in a Lindemann capillary. A crystal of **8** having the approximate dimensions 0.600 × 0.200 × 0.200 mm was mounted in a similar way. The X-ray diffraction data were collected using an Enraf Nonius CAD4A diffractometer with graphite-monochromated Cu Kα radiation. Both crystals were very weak diffractors which resulted in a lack of high angle diffraction data. Unit cell parameters were determined by a least-squares analysis of 25 automatically centered reflections in the range 15° < 2θ < 22°. Data were collected at 23 ± 1 °C using the $\omega/2\theta$ scan technique with full details presented in Table 1.

The data analysis and refinement was carried out with the programs of the TEXSAN software package. Both structures were solved by using direct methods and the non-hydrogen atoms were refined anisotropically. The N-bonded hydrogen atoms in the structure of **8** were refined. All other H-atoms were assigned calculated positions and were included in the final full-matrix refinement.
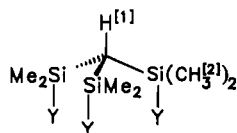
**Figure 2.** Numbering of the ^{1}H nuclei in the trisilylmethane units.

Table 2. ^{1}H-NMR Data of Functionalized Trisilylmethanes

compound	$\delta(H^2)$	$\delta(H^1)$
HC(SiMe$_2$H)$_3$ (A)^{a,b}	0.05	−0.88
HC(SiMe$_2$Br)$_3$ (B)^{a,b}	0.67	0.25
HC{SiMe$_2$NH(4-CH$_3$C$_6$H$_4$)}$_3$ (1)^a	0.47	0.83
HC{SiMe$_2$NH(3-CH$_3$C$_6$H$_4$)}$_3$ (2)^a	0.45	0.77
HC{SiMe$_2$NH(2-CH$_3$C$_6$H$_4$)}$_3$ (3)^a	0.43	0.92
HC{SiMe$_2$NH(C$_6$H$_5$)}$_3$ (4)^a	0.46	0.93
HC{SiMe$_2$NH(4-FC$_6$H$_4$)}$_3$ (5)^a	0.37	0.80
HC(SiMe$_2$NHMe)$_3$ (6)^c	0.45	−0.30
HC(SiMe$_2$NH^{t}Bu)$_3$ (7)^{a,b}	0.37	−1.25
HC{SiMe$_2$NH[CH(CH$_3$)C$_6$H$_5$]}$_3$ (8)^d	0.13; 0.24	−0.88
HC[SiMe$_2$N(Li)^{t}Bu]$_3$ (9)^d	0.43	−1.14
HC{SiMe$_2$N(Li)(4-CH$_3$C$_6$H$_4$)}$_3$·2Et$_2$O (10)^d	0.47	−0.83
HC{SiMe$_2$N(Li)(3-CH$_3$C$_6$H$_4$)}$_3$·2Et$_2$O (11)^d	0.55	−0.81
HC{SiMe$_2$N(Li)[CH(CH$_3$)C$_6$H$_5$]}$_3$·2THF (12)^d	0.16; 0.27	−0.72

^{a} Recorded in CDCl$_3$. ^{b} From ref 12. ^{c} From ref 20. ^{d} Recorded in C$_6$D$_6$.

Results and Discussion

Preparation of the Trisilylmethane-Derived Tris(arylamines) HC(SiMe$_2$NHAr)$_3$ (Ar = Substituted Phenyl Groups). The aminolysis of HC(SiMe$_2$Br)$_3$, a compound first characterized by Eaborn and co-workers,[18] with primary aryl amines in diethyl ether in the presence of triethylamine as auxiliary base yielded a whole series of secondary triamines derived from trisilylmethane (reaction 1). The conversion proceeded smoothly provided the

$$\text{HC(SiMe}_2\text{Br)}_3 \xrightarrow[\text{- HNEt}_3\text{Br}]{\text{3 H}_2\text{NAr, NEt}_3} \qquad (1)$$
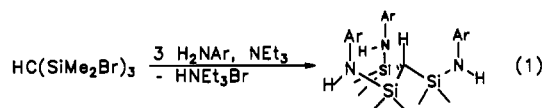
Ar = 4-CH$_3$C$_6$H$_4$: 1 ; C$_6$H$_5$: 4
Ar = 3-CH$_3$C$_6$H$_4$: 2 ; 4-FC$_6$H$_4$: 5
Ar = 2-CH$_3$C$_6$H$_4$: 3

primary amine was sufficiently nucleophilic, a requirement established by the almost complete inertness of the trisbromosilane toward perfluoroaniline C$_6$F$_5$NH$_2$. Steric factors do not appear to be relevant in this case in view of the high reactivity toward, for instance, t-BuNH$_2$.[18] The formulation of the aminofunctionalized trisilylmethanes was established by elemental analysis. The amines 1–5 were obtained as highly crystalline colorless solids which are very soluble in polar aprotic solvents and aromatic hydrocarbons but only sparingly so in saturated hydrocarbons. In contrast to the previously characterized amines HC(SiMe$_2$NHR)$_3$ [R = Me (6),[20] t-Bu (7)[12]], which readily underwent thermal RNH$_2$ extrusion if heated above ambient temperature, compounds 1–5 show a considerable thermal stability and melt without decomposition.

NMR Spectroscopy of 1–5: Preferred Conformations of the Tris(arylamines) in Solution. The spectroscopic data (^{1}H-, ^{13}C-, ^{29}Si, ^{19}F-NMR) of 1–5 are consistent with an effective 3-fold molecular symmetry, as would be expected for the formulations given above. However, in comparison to the previously characterized trisilylmethane derivatives, the ^{1}H-NMR resonance of the proton bonded to the bridgehead carbon atom, HC(Si···)$_3$, in the central unit is observed at considerably lower field than expected, a situation which deserved closer inspection. The chemical shifts of these signals (H^1) as well as those of the resonances of the (CH$_3$)$_2$Si protons (H^2) (Figure 2) are listed in Table 2 along with the corresponding data of related compounds. The resonances of the H^2 nuclei appear within the expected range, the electron-withdrawing properties of the Br-substituent in **B**

Table 3. Temperature-Dependence of the Chemical Shift of the H^1 Resonance in **1** (Recorded in Toluene-d_8)

	T (K)								
	235	245	265	295	315	325	335	345	355
$\delta(H^1)$	1.38	1.35	1.17	0.91	0.77	0.72	0.67	0.63	0.59

being responsible for the shift to lower field ($\delta = 0.67$). The same argument applies to the chemical shift of the H^1 nucleus in this compound. However, the above-mentioned unusual position of the signals assigned to H^1 in 1–5, which are shifted by up to 2.1 ppm to lower field in comparison to **7** may not be explained by through-bond operating electronic effects. An additional feature is a strong temperature dependence of the chemical shift of the H^1 signal in the aryl-substituted amines (not observed for 7!). In 1, for example, $\delta(H^1) = 1.38$ at 235 K (recorded in toluene-d_8) and is shifted to $\delta(H^1) = 0.59$ at 355 K (Table 3) while the other resonances in the molecule are barely affected. The ^{1}H-NMR spectra of the amines 2–5 display a similar, although somewhat less pronounced, temperature dependence of the respective H^1 signal. Both the temperature dependence and the unusual chemical shift of the apical proton may be explained by the assumption of a thermodynamically preferred conformation (or at least subspace within the complete space of possible conformations) in solution in which the trisilylmethane backbone is folded "inside-out" (as shown in eq 1) with respect to the adamantoid arrangement established for HC(SiMe$_2$N(Li)tBu)$_3$ (9), thereby bringing H^1 into close proximity of the aryl groups. This situation, in which this ^{1}H nucleus is shifted by the ring currents of the aryl units, is populated ("frozen out") by lowering the temperature. In order to obtain additional information concerning the conformations of these molecules in solution ^{1}H-NOESY spectra of 1–5 were carried out at variable temperatures.[22] The mixing times chosen were $t_{mix} = 0.5$, 1.5, and 3.0 s, of which $t_{mix} = 1.5$ s was found to be ideal for the observation of NOE cross peaks in the spectra. Again, the most conclusive data were obtained for **1**. A ^{1}H-NOESY spectrum of **1** recorded in C$_6$D$_6$ at 280 K is shown in Figure 3. The most remarkable spectral feature is the absence of a non-diagonal peak between H^1 and H^2, a characteristic of e.g. **6** and **7** in solution, which indicates that both types of nuclei are not "pointing at each other", i.e. are not at close proximity in the preferred conformation of the molecule (the absence of this cross-peak due to potential "leakage" through cross relaxation between the equivalent nuclei of the CH$_3$ groups[23] is unlikely in view of the observed peak between, for instance, H^5 and H^6). On the other hand, H^1 and H^4 show cross relaxation and are therefore probably close to each other [the equivalence of the two o- and m-H positions is a consequence of a rapid rotation of the tolyl groups on the NMR(chemical shift) time scale]. This is indeed the expected result for a preferred conformation ("inside out") as postulate above.

On warming solutions of **1** to above 310 K the absent set of cross-peaks between H^1 and H^2 appears out of the spectral noise, a consequence of the thermal population of less favored conformational states in which both nuclei are closer to each other. In the same experiment performed for 7, 8 (*vide infra*), and 9, strong cross relaxation between H^1 and H^2 is to be seen as a consequence of the preference of an "adamantane" related geometry of the molecule in solution.

The NOESY experiments performed for 2, 4, and 5 gave essentially similar results (NOE networks) as those of 1 although the situation is somewhat less clear for the o-tolyl-substituted amine 3 in which the H^1–H^2 cross-peak may be (weakly) observed even at 260 K.

(22) Ernst, R. R.; Bodenhausen, G.; Wokaun, A. *Principles of Nuclear Magnetic Resonance in One and Two Dimensions*, Clarendon Press: Oxford, England, 1987.

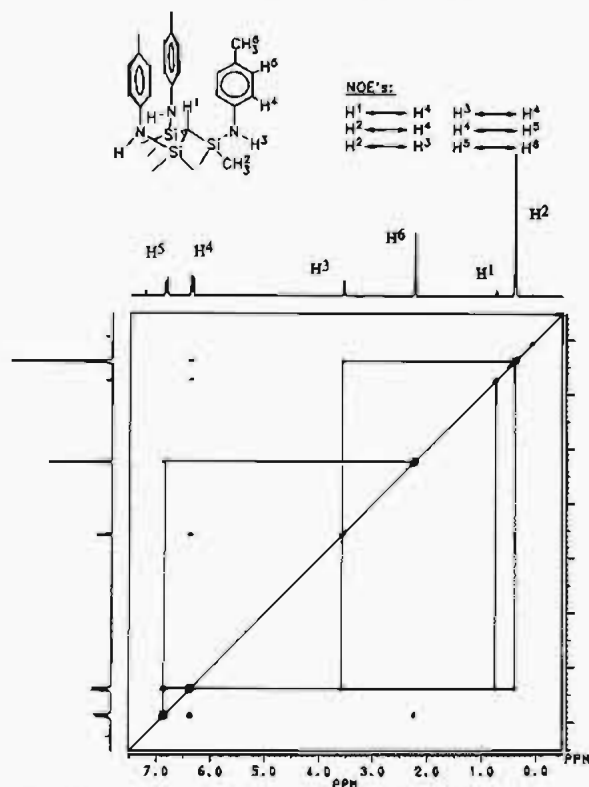(23) Keepers, J. W.; James, T. L. *J. Magn. Reson.* **1984**, *57*, 404.

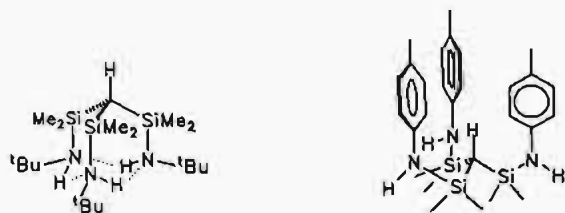**Figure 3.** ¹H-NOESY spectrum of **1** recorded at 280 K in C₆D₆. t_{mix} = 1.5 s.

Figure 4. The two conformational extremes postulated in order to account for the spectroscopic properties of **1–8** in solution.

The preferred conformations of **1–7** in solution may be described as lying between the two extremes depicted in Figure 4: (a) a conformation related to the adamantane structure of HC-[SiMe₂N(Li)*t*Bu]₃ (**9**) which may be enhanced by weak N–H···N hydrogen bonding proposed to dominate for **7**; (b) a conformation in which the trisilylmethane framework is folded "inside out", as is postulated to represent the preferred arrangement in **1–5**, resulting in a close proximity between the apical proton H¹ and the anisotropy cones of the aryl groups.

Solid-State Structures of 1–5. X-ray Structure Analysis of 1. The ν(N-H) bands in the infrared spectra of **1–5** recorded as KBr pellets lie in the range 3380–3420 cm⁻¹ and are therefore shifted toward higher wavenumbers in comparison to those of **6** and **7** (3370 and 3290 cm⁻¹, respectively[12,20]). This may be a consequence of a different degree of N–H···N association in the aryl and alkyl amines in the solid state, indicating a possible intramolecular hydrogen bonding interaction in the latter type of compounds. In order to establish the overall molecular arrangement of the aryl amines in the solid a single-crystal X-ray structure analysis of **1** was carried out. Although crystals of the amines diffracted only poorly, the basic features of the structure of **1** were obtained in the crystallographic study. The molecular structure of **1** is depicted in Figure 5, selected bond lengths and interbond angles are given in Table 4, and the fractional coordinates are listed in Table 5.

The molecular structure in the crystal bears close resemblence to the preferred arrangement in solution postulated in the previous
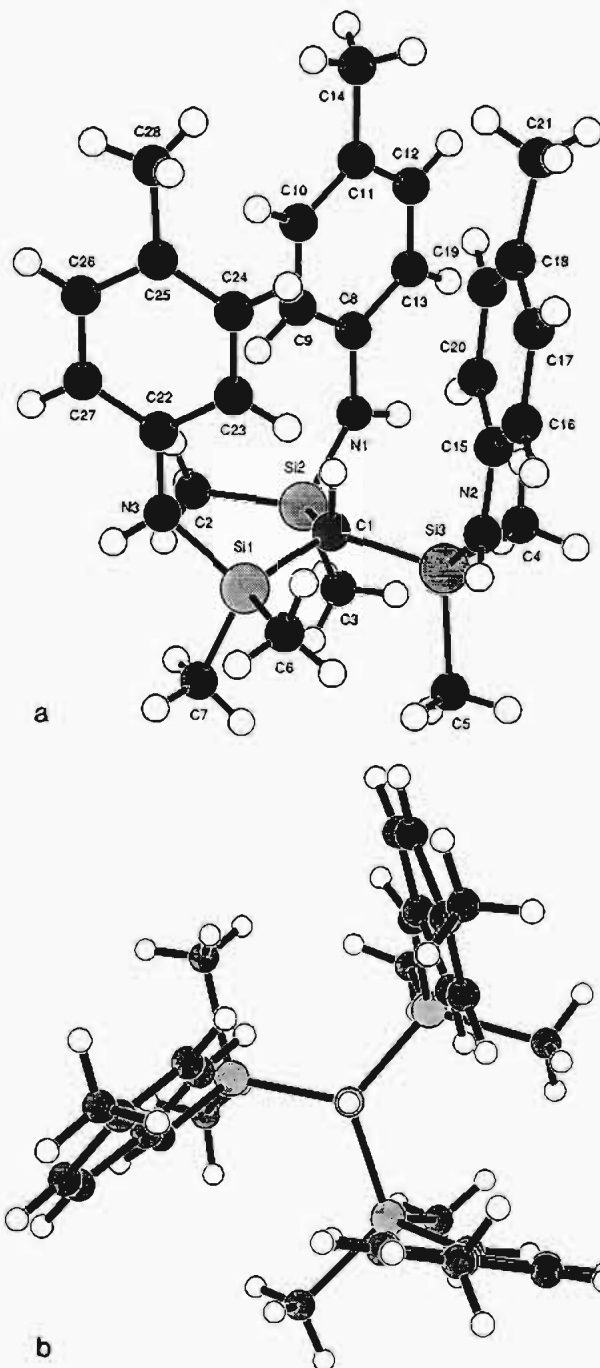
Figure 5. (a) Molecular structure of **1** in the crystal. (b) View along the idealized molecular 3-fold axis.

section. The molecule has idealized C_3-symmetry and an overall geometry which is characterized by the trisilylmethane unit being turned almost "inside out" with respect to an adamantoid structure. The orientation of the SiMe₂ moieties is not completely inverted with respect to that found in **7** but significantly twisted, probably due to steric repulsion of the methyl groups. Three of these adopt what may be termed "axial" positions while the others occupy "equatorial" positions. As a consequence, the tolyl–N atoms are somewhat displaced relative to the H(1)–C(1)–Si planes (Figure 5b). The apical proton at the bridge head carbon atom is embedded in a pocket defined by the tolyl groups. The Si–C bond lengths in the molecule lie in the range [1.866(8)–1.887(8) Å] found for related compounds.

The geometry of the tolyl–NH–Si unit is obviously of greatest interest and, in spite of the less than desired quality of the diffraction data, is reasonably well defined. The Si–N distances between 1.72(1) and 1.77(1) Å are comparable to those of other

Table 4. Selected Bond Lengths (Å) and Interbond Angles (deg) for **1**

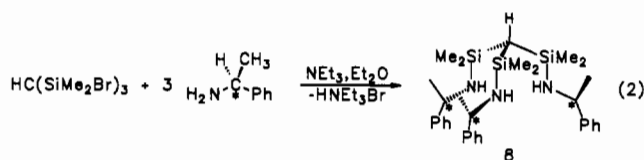|			
Si(1)–N(3)	1.73(1)	Si(2)–C(3)	1.86(1)
Si(1)–C(1)	1.866(8)	Si(3)–N(2)	1.77(1)
Si(1)–C(6)	1.88(1)	Si(3)–C(1)	1.873(8)
Si(1)–C(7)	1.860(8)	Si(3)–C(4)	1.86(1)
Si(2)–N(1)	1.72(1)	Si(3)–C(5)	1.86(1)
Si(2)–C(1)	1.887(8)	N(1)–C(8)	1.40(1)
Si(2)–C(2)	1.87(1)		
N(3)–Si(1)–C(1)	110.7(4)	C(2)–Si(2)–C(3)	107.0(4)
N(3)–Si(1)–C(6)	108.3(4)	N(2)–Si(3)–C(1)	108.8(4)
N(3)–Si(1)–C(7)	105.7(6)	N(2)–Si(3)–C(4)	107.6(5)
C(1)–Si(1)–C(6)	113.0(4)	N(2)–Si(3)–C(5)	106.5(6)
C(1)–Si(1)–C(7)	112.4(4)	C(1)–Si(3)–C(4)	114.2(4)
C(6)–Si(1)–C(7)	106.3(4)	C(1)–Si(3)–C(5)	111.3(3)
N(1)–Si(2)–C(1)	108.9(4)	C(4)–Si(3)–C(5)	108.1(4)
N(1)–Si(2)–C(2)	108.5(5)	Si(1)–C(1)–Si(2)	115.9(4)
N(1)–Si(2)–C(3)	106.0(7)	Si(1)–C(1)–Si(3)	116.5(4)
C(1)–Si(2)–C(2)	114.1(4)	Si(2)–C(1)–Si(3)	115.7(4)
C(1)–Si(2)–C(3)	112.0(4)		

Table 5. Fractional Atomic Coordinates of **1**

atom	x	y	z
Si(1)	0.7417(3)	0.2763(4)	0.95566(8)
Si(2)	1.0196(3)	0.1923(3)	0.9115(1)
Si(3)	0.8202(4)	0.4527(3)	0.88312(8)
N(1)	1.043(1)	0.124(1)	0.8670(3)
N(2)	0.638(1)	0.472(1)	0.8638(3)
N(3)	0.684(1)	0.106(1)	0.9645(4)
C(1)	0.8358(8)	0.2830(8)	0.9105(2)
C(2)	1.043(1)	0.046(1)	0.9471(3)
C(3)	1.174(1)	0.318(1)	0.9219(3)
C(4)	0.941(1)	0.463(1)	0.8431(3)
C(5)	0.860(1)	0.6075(9)	0.9146(3)
C(6)	0.579(1)	0.397(1)	0.9554(3)
C(7)	0.865(1)	0.327(1)	0.9978(2)
C(8)	0.953(2)	0.030(2)	0.8453(8)
C(9)	0.837(4)	−0.039(3)	0.8598(3)
C(10)	0.746(2)	−0.128(2)	0.837(1)
C(11)	0.766(3)	−0.150(1)	0.7999(8)
C(12)	0.882(4)	−0.082(3)	0.7854(4)
C(13)	0.972(2)	0.008(2)	0.807(1)
C(14)	0.663(2)	−0.247(1)	0.7763(4)
C(15)	0.548(3)	0.391(1)	0.8385(4)
C(16)	0.402(2)	0.413(2)	0.8265(5)
C(17)	0.333(2)	0.323(2)	0.7997(5)
C(18)	0.410(3)	0.211(2)	0.7853(4)
C(19)	0.552(2)	0.190(2)	0.7975(6)
C(20)	0.621(1)	0.279(2)	0.8234(5)
C(21)	0.316(1)	0.129(1)	0.7540(4)
C(22)	0.584(2)	0.019(2)	0.9440(6)
C(23)	0.516(2)	0.068(1)	0.9101(7)
C(24)	0.415(2)	−0.015(3)	0.8888(4)
C(25)	0.377(1)	−0.147(3)	0.9004(7)
C(26)	0.443(3)	−0.198(1)	0.9341(8)
C(27)	0.544(2)	−0.115(3)	0.9557(4)
C(28)	0.262(1)	−0.240(1)	0.8789(4)

aryl amines.[24-26] The coordination geometry at the silicon atoms is distorted tetrahedral, the interbond angles ranging from 106(1) to 112(1)°. The Si–N–C$_\alpha$(tolyl) angle [129(1)–133(1)°] is larger than expected for sp²-hybridized nitrogen, however, not unexpectedly so in view of the low steric demand of the third substituent (H) at the N-atom.

The torsional angle of the aryl groups relative to the plane defined by Si, N, and C$_\alpha$(tolyl) was found to lie between 3 and 11° (Figure 5b) enabling a good overlap between the aromatic π-system with the p-orbital at the nitrogen atom, a situation which

(24) Shelrick, W. S. In *The Chemistry of Organic Silicon Compounds*; Patai, S., Rappoport, Z., Eds.; Wiley: New York, 1989; p 227.
(25) Lukevics, E.; Pudova, O.; Sturkovich, R. *Molecular Structures of Organosilicon Compounds*; Ellis Horwood: New York, 1989; p 93.
(26) See e.g.: Glidewell, C.; Robiette, A. G.; Sheldrick, G. M. *J. Mol. Struct.* **1971**, *9*, 476. Hansen, H. D.; Mundt, O.; Kaim, W. *J. Organomet. Chem.* **1985**, *296*, 321. Martin, A. R.; Svensson, A.; Bates, R. B.; Ortega, R. B. *Acta Crystallogr., Sect. C* **1985**, *41*, 1804.

is expected to alter the electronic properties of the planar nitrogen center as well as the nature of the Si–N bond relative to alkyl-substituted species.

Synthesis, Spectroscopic Properties, and X-ray Crystal Structure Analysis of HC{SiMe$_2$NH-[(*S*)-CH(CH$_3$)Ph]}$_3$ (8). Condensation of HC(SiMe$_2$Br)$_3$ with *(S)*-(1-phenylethyl)amine under the same conditions as described above for arylamines gives, after recrystallization of the crude product from pentane, the chiral triamine HC{SiMe$_2$NH[(*S*)-CH(CH$_3$)Ph]}$_3$ (**8**) in good yield (reaction 2). In contrast to the syntheses of the neopentane-

derived amines H$_3$CC(CH$_2$NHR)$_3$ which are based on the functionalization of a primary amine H$_3$CC(CH$_2$NH$_2$)$_3$ and are thus limited in their scope by the preparative methods available,[11] the condensation of a primary amine with an "activated" ligand backbone represents a simple route to chiral tripodal amines.

The ¹H-, ¹³C-, and ²⁹Si-NMR spectra are again consistent with an effective 3-fold symmetry of the system as implied by the formulation derived from the analytical data. The ¹H resonance of the apical proton (H¹) is observed at δ = −0.88 (recorded in C$_6$D$_6$) in a similar range as the other known alkyl amines. The signals of the diastereotopic methyl groups at the silicon atoms appear at δ = 0.13 and 0.24. In the ¹H-¹H-NOESY spectra recorded of the compound (t_{mix} = 1.5; 3.0 s; *T* = 280 K), an intense cross-peak between the protons of the SiMe$_2$ groups H² and H¹ is found, while cross relaxation between H¹ and protons of the ligand periphery is not observed. The ν(N–H) band in the IR spectrum at 3343 cm⁻¹ (KBr) indicates a certain degree of intra-(or possibly inter-) molecular hydrogen bonding.
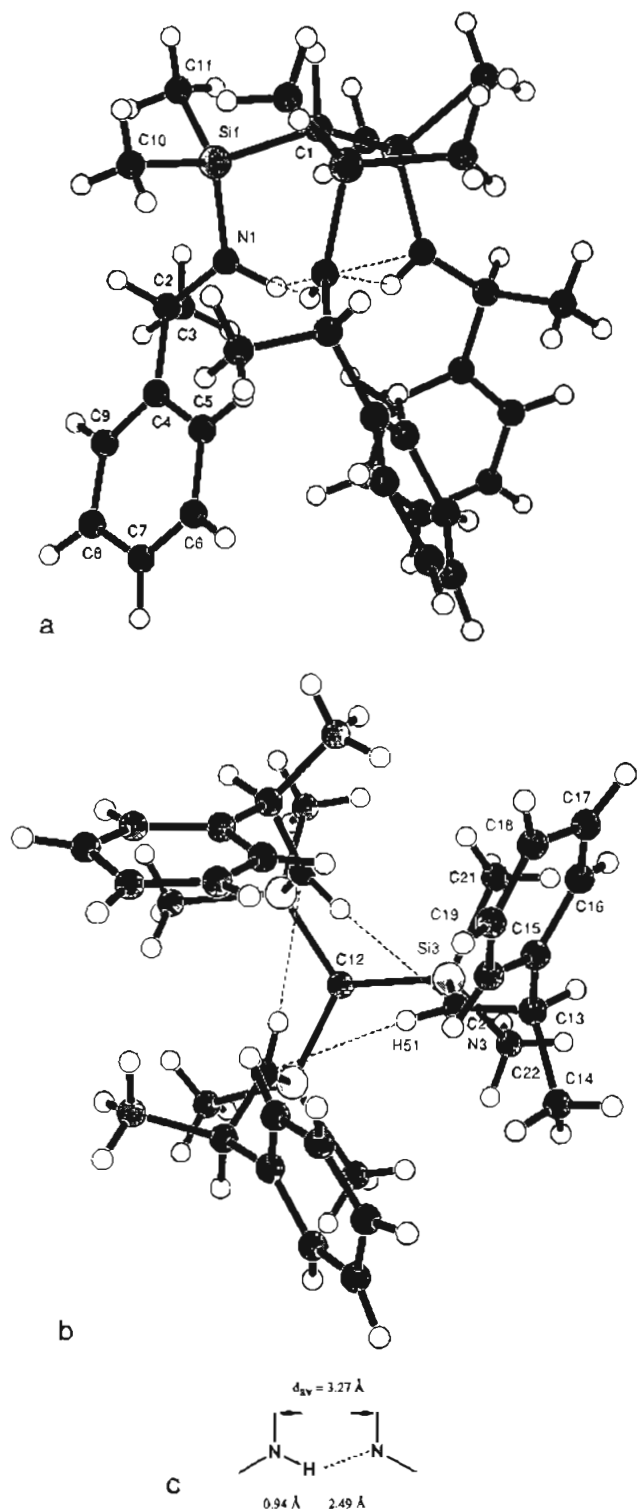
In order to obtain a more detailed picture of the molecular structure of **8** in the solid state a single-crystal X-ray structure analysis of the compound was carried out. A view of the molecular structure of **8** is given in Figure 6, selected bond distances and interbond angles are given in Table 6 and the fractional coordinates of **8** are listed in Table 7.

Similar to the crystals of **1**, those of **8** were weak diffractors. Nevertheless, the overall structure of the compound is well established on the basis of the data obtained. The arrangement of the ligand backbone of **8** in the crystal is closely related to that found in the crystal structure analysis of HC[SiMe$_2$N(Li)*t*Bu]$_3$ (**9**). Instead of the lithium atoms in the latter, the N-bonded protons, which were directly localized in the difference Fourier syntheses and refined, appear to be part of a weakly associated (NH)$_3$ ring structure which forms the base of the distorted adamantoid cage (an interpretation supported by the position of the ν(N–H) band, *vide supra*). The geometry of the N–H···N units is shown in Figure 6c. The Si–N distances [d_{av}(Si–N) = 1.70 Å] are significantly shorter than in **1** but comparable to those of Me$_3$SiNMeH[27] and **9**. This may be a consequence of the withdrawal of electron density from the Si–N bond by the π-overlapping aryl groups in aryl(silyl)amines.

The packing of compound **8** in the unit cell of the crystal (space group *P*3) is particularly noteworthy. The unit cell contains three independent molecules two of which "point" in the same direction along the 3-fold axis while the third molecule is inverted in its orientation (Figure 7). Since there are no strong intermolecular forces (H bonds, ionic interactions, etc.) present in the crystal there is no obvious relationship between molecular structure and the packing pattern.

(27) Roper, W. R.; Wilkins, C. J. *Trans. Faraday Soc.* **1962**, *58*, 1686.

Table 6. Selected Bond Lengths (Å) and Interbond Angles (deg) for **8**

Si(1)–N(1)	1.697(9)	Si(3)–C(12)	1.857(6)
Si(1)–C(1)	1.864(6)	Si(3)–C(21)	1.85(1)
Si(1)–C(10)	1.87(1)	Si(3)–C(22)	1.89(1)
Si(1)–C(11)	1.88(1)	N(2)–C(24)	1.47(1)
Si(2)–N(2)	1.69(1)	N(2)–H(49)	0.933
Si(2)–C(23)	1.869(5)	N(1)–C(2)	1.46(1)
Si(2)–C(32)	1.83(1)	N(1)–H(50)	0.942
Si(2)–C(33)	1.87(1)	N(3)–C(13)	1.44(1)
Si(3)–N(3)	1.707(9)	N(3)–H(51)	0.940
N(1)–Si(1)–C(1)	105.4(6)	C(23)–Si(2)–C(33)	110.4(6)
N(1)–Si(1)–C(10)	107.1(6)	C(32)–Si(2)–C(33)	102.9(7)
N(1)–Si(1)–C(11)	114.8(5)	N(3)–Si(3)–C(12)	105.2(6)
C(1)–Si(1)–C(10)	115.6(5)	N(3)–Si(3)–C(21)	108.7(5)
C(1)–Si(1)–C(11)	109.4(6)	N(3)–Si(3)–C(22)	113.1(5)
C(10)–Si(1)–C(11)	104.9(6)	C(12)–Si(3)–C(21)	115.6(5)
N(2)–Si(2)–C(23)	108.4(6)	C(12)–Si(3)–C(22)	111.4(6)
N(2)–Si(2)–C(32)	108.0(6)	C(21)–Si(3)–C(22)	103.0(6)
N(2)–Si(2)–C(33)	113.8(6)	Si(2)–N(2)–C(24)	125.6(8)
C(23)–Si(2)–C(32)	113.4(5)	Si(1)–C(1)–Si(1)	113.2(4)

Table 7. Fractional Atomic Coordinates for **8**

atom	x	y	z
Si(1)	0.0941(2)	0.1192(2)	0.7697
Si(2)	–0.2593(2)	0.4583(2)	0.8822(4)
Si(3)	0.2081(2)	0.5972(2)	0.9344(4)
N(2)	–0.2760(7)	0.4670(7)	1.038(1)
N(1)	0.1167(6)	0.1099(6)	0.6158(8)
N(3)	0.2043(6)	0.6235(6)	0.7794(8)
C(1)	0	0	0.817(2)
C(2)	0.191(1)	0.184(1)	0.541(1)
C(3)	0.272(1)	0.170(1)	0.527(2)
C(4)	0.161(1)	0.201(1)	0.414(2)
C(5)	0.072(1)	0.148(1)	0.368(2)
C(6)	0.045(2)	0.162(2)	0.249(2)
C(7)	0.110(3)	0.227(2)	0.176(2)
C(8)	0.195(2)	0.283(2)	0.218(3)
C(9)	0.221(1)	0.265(1)	0.334(2)
C(10)	0.063(1)	0.2136(9)	0.780(1)
C(11)	0.197(1)	0.158(1)	0.879(1)
C(12)	¹/₃	²/₃	0.980(2)
C(13)	0.1216(9)	0.5852(8)	0.702(1)
C(14)	0.0955(9)	0.659(1)	0.671(1)
C(15)	0.124(1)	0.535(1)	0.584(1)
C(16)	0.077(1)	0.440(1)	0.580(2)
C(17)	0.076(2)	0.394(2)	0.474(3)
C(18)	0.137(3)	0.445(3)	0.377(4)
C(19)	0.179(2)	0.535(3)	0.376(3)
C(20)	0.178(1)	0.581(1)	0.482(2)
C(21)	0.1544(9)	0.469(1)	0.950(1)
C(22)	0.133(1)	0.625(1)	1.039(2)
C(23)	–¹/₃	¹/₃	0.834(1)
C(24)	–0.221(1)	0.550(1)	1.117(2)
C(25)	–0.275(1)	0.599(1)	1.146(1)
C(26)	–0.185(1)	0.5251(9)	1.233(2)
C(27)	–0.238(1)	0.494(1)	1.340(2)
C(28)	–0.205(1)	0.468(1)	1.447(2)
C(29)	–0.119(2)	0.481(1)	1.446(2)
C(30)	–0.068(1)	0.512(1)	1.341(3)
C(31)	–0.097(1)	0.536(1)	1.234(2)
C(32)	–0.1340(9)	0.505(1)	0.856(1)
C(33)	–0.285(1)	0.535(1)	0.780(1)

Figure 6. (a) Molecular structure of **8** in the crystal. (b) View along the crystallographic 3-fold axis showing the (N–H)₃ unit. (c) Geometrical details of the N–H···N interaction. The average geometrical parameters of the three independent molecules are given.

Lithiation of the Free Amines and Synthesis of HC(SiMe₂-NR)₃TiX (R = 4-CH₃C₆H₄, 3-CH₃C₆H₄, 4-FC₆H₄). Upon reaction of **1–5** and **8** with 3 molar equiv of *n*-BuLi the corresponding trilithium amides are formed. In contrast to **9** which could be fully characterized,[12] the arylamides are thermally considerably more labile and could only be studied spectroscopically as their diethyl ether solvates. As in the case of the bis-THF adduct of **9**, the ¹H- and ¹³C-NMR spectra are consistent with an effective 3-fold molecular symmetry of the lithium salt, a situation due to rapid chemical exchange of the solvating Et₂O

molecules. Of particular interest was the lithium amide derived from **1**, HC[SiMe₂N(Li)(4-CH₃C₆H₄)]₃(Et₂O)₂ (**10**), since the structure in solution of the amine was best understood (Table 2). The most notable spectroscopic feature is the chemical shift of the apical proton in the trisilylmethane unit of **10** which is at δ = –0.80 (C₆D₆, 295 K), i.e. shifted by ca. 1.6 ppm to higher field in comparison to **1**. This is in stark contrast to the behavior of the *tert*-butyl-substituted analogue in which the apical proton experiences a *downfield shift* by ca. 0.1 ppm upon lithiation. Here again, conformational changes of the molecule as a whole rather than through bond interaction are apparently responsible for the observed effect. In view of the known crystal structure
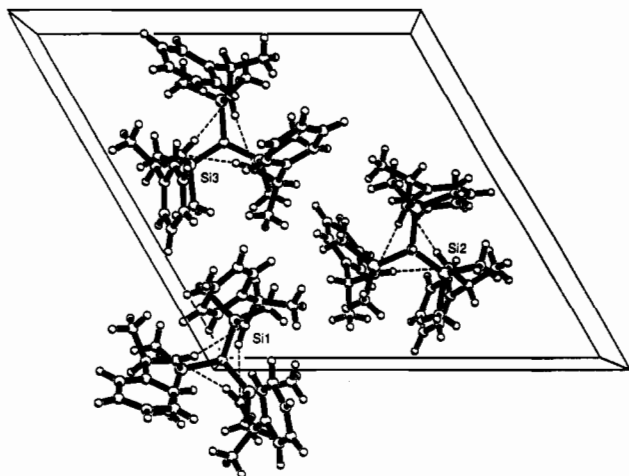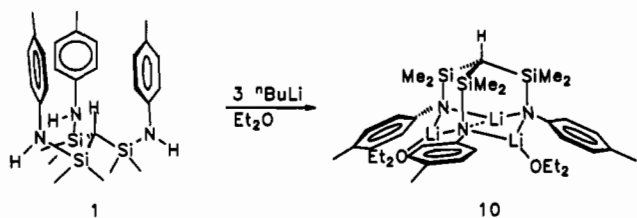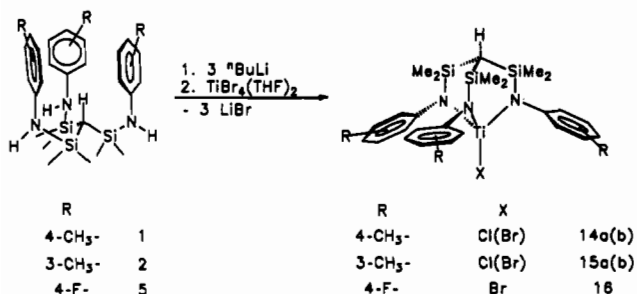
Figure 7. View of the trigonal unit cell of **8** along the *c*-axis showing the packing of the three independent molecules.

Scheme 1. Conformational Changes in the Transformation **1** → **10**

Scheme 2. Formation of the Ti–Amides **14–16**

R		R	X	
4-CH₃-	1	4-CH₃-	Cl(Br)	14a(b)
3-CH₃-	2	3-CH₃-	Cl(Br)	15a(b)
4-F-	5	4-F-	Br	16

of **9** as well as its THF adduct, the intramolecular reorientation depicted in Scheme 1 provide the best explanation of the spectroscopic data obtained. *In situ* reaction of the lithium amides $HC[SiMe_2N(Li)R]_3$ [R = 4-$CH_3C_6H_4$ (**10**), 3-$CH_3C_6H_4$ (**11**), 4-FC_6H_4 (**13**)] with $TiX_4(THF)_2$ at –50 °C and subsequent warming of the reaction mixture to room temperature give the corresponding titanium amide complexes $HC(SiMe_2NR)_3TiX$ in yields ranging between 20 and 55% (Scheme 2). Since the isolation of the amides relies totally upon the crystallization of the product from the reaction mixture (after separation from the LiCl formed alongside) the yields given in this paper do not reflect the actual conversion to the desired product. ¹H-NMR studies of the product mixtures indicate a conversion of over 80% to the Ti-amides.

An important feature of the preparation of Ti–amides by reaction of titanium halides with lithium amides is the competing reduction of the tetravalent titanium to Ti(III) species. This reaction could be almost completely suppressed by choice of a Li–amide–solvent adduct which had a low solubility in the

hydrocarbon solvent used in the reactions. *In situ* generated bis(diethyl ether) adducts of the Li salts (the structures of which may be related to that of $HC[SiMe_2N(Li)t\text{-}Bu]_2\cdot2THF$, which was characterized by X-ray crystallography[12]) provide the desired heterogeneous reaction conditions and have proved to give the best results in these syntheses.

The Ti complexes are orange-red crystalline solids which are soluble in aprotic organic solvents but slowly decompose in halogenated hydrocarbons. The 3-fold symmetry of the proposed structure is shown in Scheme 2. The resonances of the ligand nuclei are shifted to lower field, a consequence of the Lewis acidity of the Ti(IV) centers to which the amides are coordinated. Single crystals of **14b** may be readily grown from diethyl ether; they crystallize with a diethyl ether molecule of solvation. Partial loss of this solvent molecule rendered the crystals unsuitable for a full and proper structure determination. However, a partial solution of the diffraction data support the structural arrangement shown above, a four coordinate Ti atom coordinated to the tripodal amido ligand and a lone bromide ligand.[28] The geometrical details will remain to be established in future investigations.

The fact that the isolation and purification of the Ti complexes relies entirely on their crystallization from the product mixtures has to date impeded the characterization of a titanium complex derivative of **8**, a compound which is of interest due to the chirality of its "reaction center" at the metal.[29] Our current activities focus upon the development of alternative methods of isolation as well as the extension of the work reported here to other early transition metals.

Conclusions

This study has established a novel type of tripodal amido ligand in transition metal coordination chemistry. The structural investigations of the amine precursors, the lithiated amide transfer reagents and the Ti(IV) complexes have shown that upon metalation of an amino-functionalized trisilylmethane and exposure to a transition metal halide complex, the formally highly charged polydentate ligand literally wraps around a coordination hemisphere of the metal, substituting three halide ligands.

With these systems a new type of monofunctional Ti complex is available which may find use in more complex structural arrays. These species have already been successfully employed as building blocks in the generation of thermally stable early–late hetero-bimetallics containing unsupported highly polar metal–metal bonds.[10]

Supplementary Material Available: Text detailing the structure determination and tables of crystallographic data, the positional and thermal parameters, interatomic distances, angles and torsion angles for **1** and **8** (50 pages). Ordering information is given on any masthead page.

(28) Compound **14b** crystallizes as a diethyl ether solvate. Partial loss of the diethyl ether rendered the crystals unsuitable for a full structure analysis: Complex **14b**: diethyl ether, $C_{32}H_{50}BrN_3OSi_3Ti$, monoclinic, $P2_1/c$, $a = 9.721(2)$ Å, $b = 21.784(4)$ Å, $c = 17.729(3)$ Å, $\beta = 103.8(1)°$, $Z = 4$, 634 observations with $I > 3\sigma(I)$, $R = 0.124$ for an isotropic refinement. The diethyl ether occupancy was about 50%.

(29) Note added in proof: We have now succeeded in coordinating **8** to several tetravalent early transition metals by slightly changing the reaction procedure. These results will be reported elsewhere (Memmler, H.; Gade, L. H.; Lauher, J. W. To be published).